The Localized Interplay Between Star Formation and Gas Chemistry in Nearby Starburst Galaxies

David S. Meier[1], Jean L. Turner[2] and Sara C. Beck[3]

ABSTRACT

We discuss high resolution (∼25-75 pc) imaging of the nuclear chemistry in the IR bright, nearby spirals, IC 342 and Maffei 2. Attention is focused on comparing molecular gas PDR and shock tracers, C_2H and CH_3OH, respectively, with the MIR PAHs, H_2 and atomic spectral features. C_2H is found to be a privileged tracer of the locations of PDRs. In IC 342 the PDRs are highly confined (∼50 pc scales), but less so in Maffei 2. In both nuclei the morphology of the mid infrared PAH emission is tightly correlated with the C_2H. Grain species like CH_3OH are common in spiral nuclei, but their locations do not correlate with embedded star formation and its interactions with the molecular gas. They originate, instead, at the locations of orbital resonances in the nuclear potential. The distribution of warm H_2 in IC 342 correlates better with the shocks traced by methanol emission than with PDRs. In Maffei 2 the PDR heating is favored for H_2.

Subject headings: galaxies: ISM — infrared: ISM — ISM: molecules — galaxies: individual (IC 342, Maffei 2)

1. Introduction

Massive star formation in starbursts injects large amounts of energy and momentum into the surrounding molecular ISM. The energy can change gas excitation, generate PDRs and

[1]Jansky Fellow: National Radio Astronomy Observatory, P. O. Box O, 1003 Lopezville Road, Socorro, NM 87801; email: dmeier@nrao.edu

[2]Department of Physics and Astronomy, UCLA, Los Angeles, CA 90095-1547; email: turner@astro.ucla.edu

[3]Department of Physics and Astronomy, Tel Aviv University, Ramat Aviv, Israel email: sara@wise1.tau.ac.il

trigger shocks. Gas chemistry responds to this stimuli profoundly, providing a powerful probe for characterizing the evolution of the ISM in the presence of such bursts. Spectral features in the mid infrared (MIR) such as PAHs and H_2 emission and the rotational transitions of molecules in the millimeter provide complementary insights on these chemical changes. Improvements in millimeter interferometers together with the launch of *Spitzer* permit for the first time comparisons of gas and dust chemistry on GMC scales in nearby galaxies.

2. Observations

IC 342 and Maffei 2 represent two of the closest ($D_{mpc} \simeq 3.3$ Mpc) spiral galaxies with strong nuclear star formation. The face-on IC 342 and the nearly edge-on Maffei 2 make up the two brightest members of the IC 342/Maffei group. Both are some of the brightest IR and CO sources in the sky. The nuclear molecular of each galaxy is characterized by a 'mini-spiral' terminating on a central ring set up in response to a barred potential (e.g. Meier & Turner 2001, Meier & Turner 2008). GMCs at the intersections of the arms and the central ring are the sites of the youngest starbursts. We observed seven lines at 3 mm towards the central $1'$ of IC 342 with the OVRO millimeter interferometer. Transitions from C_2H, HNCO, HNC, HC_3N, CH_3OH, $C^{34}S$, and N_2H^+ were observed. Towards Maffei 2, the same subset of transitions were mapped with the OVRO and BIMA millimeter interferometers. The C_2H and CH_3OH maps in IC 342 have resolutions of $\sim 5-6''$ (see Meier & Turner 2005 [MT05] for details), while those in Maffei 2 have resolutions of $\sim 6-8''$.

Imaging of important spectral features between 5 - 20μm was carried out in IRS mapping mode with the *Spitzer Space Telescope* [project ID: 20607]. For both galaxies spectra were obtained with SL, LL, SH and LH slits, but we only discuss the SL1, SL2 and LL2 data here. The short wavelength maps cover the same field as the millimeter maps ($\sim 70''$) while the longer wavelength maps cover $\sim 120''$. Data were preprocessed with the S15 version of the SSC pipeline. The Cubism software package (Smith et al. 2007) was used to mask bad data, build spectral cubes and extract maps of selected features. Towards selected GMCs in each nucleus spectra from 9" apertures were generated and fitted using PAHFIT.

3. Results and Discussion

3.1. Differentiated Molecular Gas Chemistry in IC 342 and Maffei 2

Our recent study of gas chemistry in IC 342 revealed striking morphological variations between different chemical tracers and identified groups of molecules that are correlated by

location and formation mechanism (MT05). A principle component analysis revealed that much of the observed chemical differentiation can be ascribed to two classes of species with distinct distributions. Here we focus on emission from the low lying C_2H(1–0, 3/2 – 1/2) and $CH_3OH(2_k - 1_k)$ transitions as representative tracers of each class of morphologies. Figures 1 and 2 show C_2H and CH_3OH imaged at 3 mm, for IC 342 and Maffei 2, respectively. In both systems C_2H and CH_3OH are nearly anti-correlated and must trace separate chemistries.

In localized Galactic environments C_2H is expected to trace dense, molecular PDRs since it forms as a daughter species of C^+, an ion abundant in the partially ionized surfaces of molecular clouds (e.g. Sternberg & Dalgarno 1995). With the achieved spatial resolution we can examine where C_2H is located with respect to the star formation to test whether this idea carries over to external galaxies. In IC 342, C_2H is localized to the inner faces of the central ring molecular clouds, particularly GMC A (see Figs. 1 and 2 for GMC designations). C_2H emission is near but not coincident with the young starburst regions seen at the ring-molecular arm intersections (GMC B and C). That this transition does not peak at the main starburst (B) suggests several scenarios for the evolution of star formation in IC 342. (1) The star forming regions are so young that the UV radiation has yet to break out of their molecular cores, while the radiation source driving the PDRs come from the somewhat older nuclear cluster centered inside the molecular ring (Böker et al. 1997). (2) GMC A is in a more diffuse state compared to the starburst GMCs due either to tidal shredding this close to the nucleus (MT05) or possibly to an interaction with the modest wind seen in this direction (Schinnerer et al., in prep.) leading to an internal cloud structure more porous to UV radiation. (3) C_2H does not in fact trace PDRs on these large (> GMC) scales.

In Maffei 2, C_2H is more extended than in IC 342, as is young star formation (Turner & Ho 1994). The starburst GMC (D+E) dominates the C_2H morphology (Fig. 2a). Fainter extended C_2H emission is observed to avoid the other CO peaks. This suggests that faint C_2H also originates from the cloud surfaces. Further evidence favoring a PDR origin of C_2H in Maffei 2 comes from an observed correlation between C_2H and the HCO^+(1–0)/N_2H^+(1–0) ratio (Meier & Turner, in prep.). Since C^+ can form HCO^+ but only destroys N_2H^+, the correlation implies C^+ distribution must follow C_2H.

A very different picture of these nuclei appear when imaging CH_3OH emission. From Galactic studies it is well known that CH_3OH is formed in icy grain mantles with no known gas phase pathways sufficiently rapid to explain the observed abundances (e.g. Millar et al. 1991). High gas phase abundances of CH_3OH evidently reflect a significant release of mantle ices into the gas phase by some heating mechanism. Heating due to star formation or shocks are the two most likely causes. If C_2H is indeed tracing PDRs, the fact that CH_3OH differs so dramatically from C_2H rules out star formation as the culprit in these starburst nuclei.

MT05 have argued from this that in these barred galaxies the injection method for CH_3OH is shocks associated with orbital resonances. In IC 342, CH_3OH traces the leading edge of bar arms, with the bar ends having especially enhanced abundances

The picture of the proposed chemical structure in IC 342 is schematically represented in Fig. 1b (Fig. 10; MT05). Remarkably, Maffei 2's basic chemical structure is consistent with an identical, but more highly inclined, version of IC 342 (Fig. 2b).

3.2. Spitzer: The Connections Between Gas Chemistry and Dust Chemistry

The MIR features accessible to *Spitzer* are also sensitive to shocks and PDRs. Direct, high resolution comparisons of the gas chemistry sampled in the MIR to the millimeter provide additional insights into the validity of the above model for these two galaxies.

Figs. 3 and 4 show the IRS maps of selected MIR spectral features. Accounting for differences in SNR, the PAH bands, particularly 7.7 μm, correlate very well with C_2H emission in both cases. GMC A is brightest in IC 342 and the starburst site in Maffei 2. This is direct confirmation that both C_2H and PAHs trace PDRs with high fidelity. *Spitzer* also reveals for the first time the weak PDRs associated with the small amount of star formation on the leading edge of the bar and the two extra-nuclear clusters in IC 342 (Fig. 3h).

In IC 342, the higher ionization states, [Ne III], [S IV] and [O IV] (not shown) have peaks near the center of the nuclear ring *not* at the site of the HII regions associated with the starburst (see for example [Ar II]). This suggests that the radiation field of the central cluster remains hard or, more speculatively, that a weak AGN as yet unseen at other wavelengths may be present. This supports scenario (1) for the source of PDR radiation in IC 342.

The H_2 S(1) morphology in IC 342 differs from the PAH and C_2H maps, extending well beyond the central ring. Evidently warm H_2 emission in IC 342 is not excited by PDR emission (at least the dominant ones), unlike what is expected (e.g. Hollenbach & Tielens 1997, Roussel et al. 2007). H_2 S(1) is much better correlated with the overall molecular gas distribution and with the grain species CH_3OH, in particular. Along the northern arm H_2 S(1) slightly leads the CH_3OH emission, which in turn leads the $^{12}CO(1–0)$ emission (MT05). The H_2 S(3)/H_2 S(1) ratio, indicates hot H_2 in IC 342, with T$\sim$ 310 K along the outer arms increasing to >510 K towards the starburst site. The hot gas fraction ranges from 20% down to 1% of the cold H_2 [estimated from CO(1–0)] in the starburst region. The H_2 S(1) emission in IC 342 thus appears to trace molecular gas heated in the bar shocks rather than PDRs. In Maffei 2, the situation is less clear. The S(1) emission is slightly more extended that the 7.7 μm PAH, but there is still good agreement between the maps. The bright C_2H emission

is also more extended, consistent with PDR conditions. H_2 temperatures are also ∼50 K lower than IC 342. H_2 S(1) is not distributed like CH_3OH in this case.

4. Summary

When spatial resolutions approaching the size of individual GMCs are reached, observations of the nuclear molecular reveal an organized and highly varied gas chemistry. The gas chemistry correlates directly with nuclear properties, tracing out the locations of PDRs and the influences of orbital dynamics.

This work is based on observations made with the *Spitzer Space Telescope*, which is operated by the Jet Propulsion Laboratory (JPL), California Institute of Technology under NASA contract 1407. Support for this work was provided by NASA and through JPL Contract 1255094. DSM acknowledges support from NSF AST-0506669 and the National Radio Astronomy Observatory which is operated by Associated Universities, Inc., under cooperative agreement with the National Science Foundation. Additional support for this work is provided by NSF grant AST-0506469 to JLT.

REFERENCES

Böker, T., Förster-Schreiber, N. M., & Genzel, R. 1997, AJ, 114, 1883

Hollenbach, D. J. & Tielens, A. G. G. M., 1997, ARA&A, 35 179

Meier, D. S. & Turner, J. L. 2001, ApJ, 551, 687

Meier, D. S. & Turner, J. L. 2005, ApJ, 618, 259

Meier, D. S., Turner, J. L. & Hurt, R. L. 2000, ApJ, 531, 200

Meier, D. S., Turner, J. L. & Hurt, R. L. 2008, ApJ, 675, 281

Millar, T. J., Herbst, E. & Charnley, S. B. 1991, ApJ, 369, 147

Roussel, H., et al. 2007, ApJ, 669, 959

Smith, J. D. T. et al., 2007a, PASP 119, 1133

Sternberg, A. & Dalgarno, A. 1995, ApJS, 99, 565

Turner, J. L., & Ho, P. T. P. 1994, ApJ, 421, 122

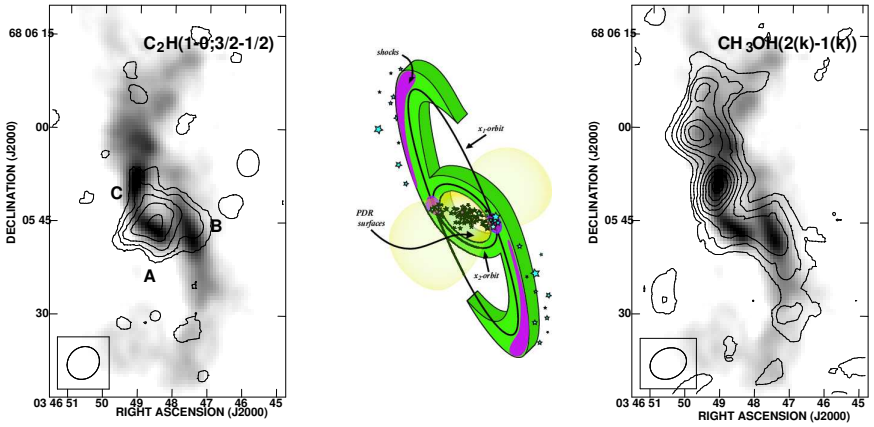

Fig. 1.— *a)* The $C_2H(1–0;3/2–1/2)$ intensity in steps of 3.0 K km s^{-1} ($5.5'' \times 4.9''$). GMC designations are labeled. *b)* A schematic of the chemical and physical structure of the nucleus of IC 342 based on the entire set of 3 mm molecular lines (Fig. 10; MT05). C_2H is an example species tracing PDR regions (yellow) while CH_3OH is a representative tracer of the bar shocks (purple). *c)* The $CH_3OH(2_k–1_k)$ intensity in steps of 1.8 K km s^{-1} ($6.0'' \times 4.8''$). In *a)* and *c)* the greyscale is I[^{12}CO(1–0)] (Meier et al. 2000).

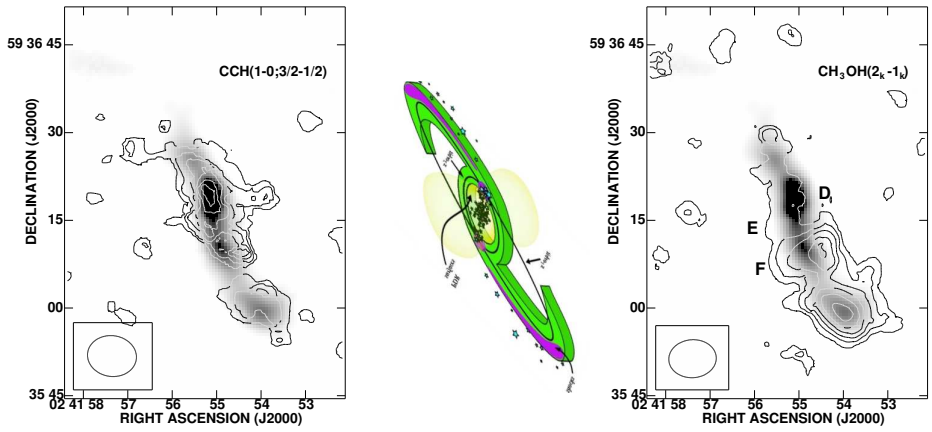

Fig. 2.— *a)* The $C_2H(1–0;3/2–1/2)$ intensity in steps of 1.1 Jy bm^{-1} km s^{-1} ($8.4'' \times 7.0''$) for Maffei 2. *b)* The chemistry schematic projected to match the geometry of Maffei 2. *c)* The $CH_3OH(2_k–1_k)$ intensity in steps of 1.5 Jy bm^{-1} km s^{-1} ($8.1'' \times 6.5''$). GMC designations are labeled. In *a)* and *c)* the greyscale is ^{13}CO(1–0) (Meier et al. 2008).

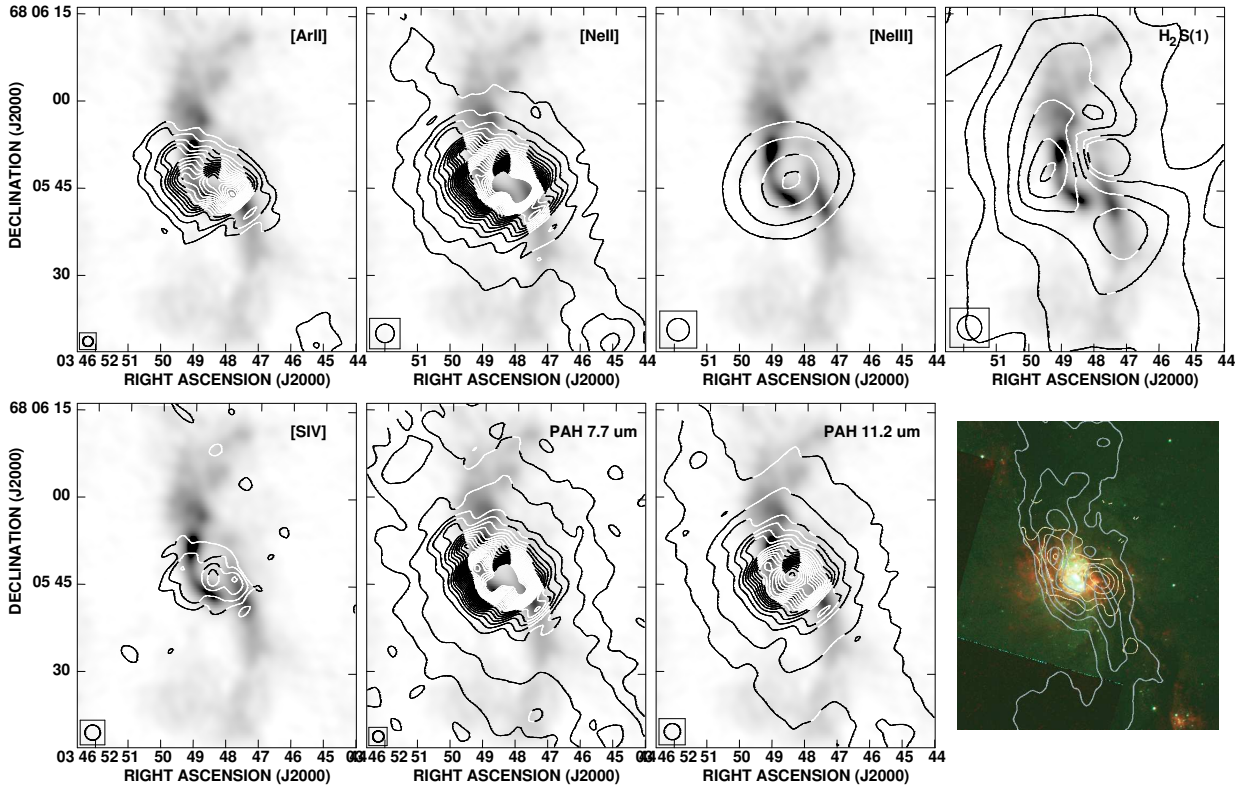

Fig. 3.— *Spitzer* IRS peak intensity maps of MIR spectral features in IC 342. Contours are spaced in steps of $A\times$ -2,-1,0.5,1,2...,25 , with *a)* $A = 15$ MJy sr^{-1} for [Ar II], *b)* $A = 30$ MJy sr^{-1} for [Ne II], *c)* $A = 30$ MJy sr^{-1} for [Ne III], *d)* $A = 4$ MJy sr^{-1} for H_2 S(1), *e)* $A = 6$ MJy sr^{-1} for [S IV], *f)* $A = 30$ MJy sr^{-1} for the 7.7μm PAH band, and *g)*$A = 30$ MJy sr^{-1} for the 11.2μm PAH band. *h)* An HST composite of IC 342's nucleus. Green is F555 and red is Hα + continuum. Blue contours are CO(1-0) and yellow contours are 3 mm (MT05).

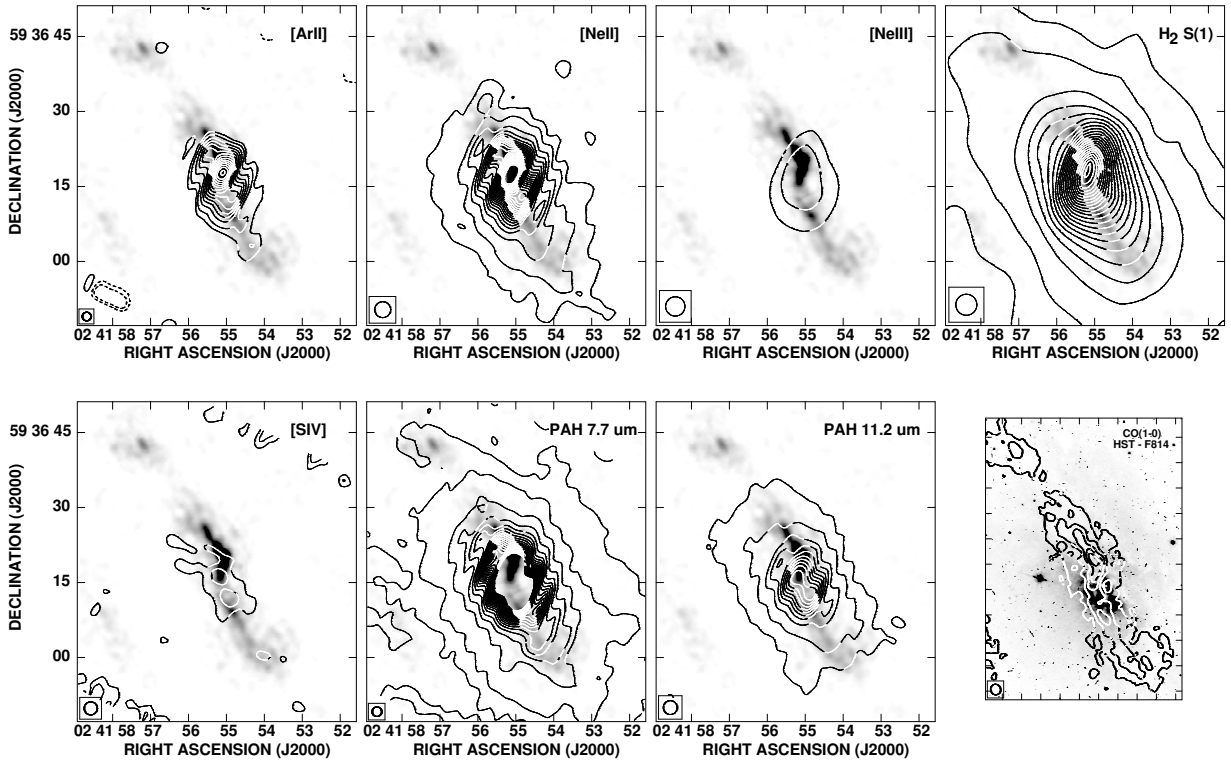

Fig. 4.— *Spitzer* IRS peak intensity maps of MIR spectral features in Maffei 2. Contours are spaced in steps of $A\times$ -2,-1,0.5,1,2...,25 , with *a)* $A = 10$ MJy sr^{-1} for [Ar II], *b)* $A = 20$ MJy sr^{-1} for [Ne II], *c)* $A = 20$ MJy sr^{-1} for [Ne III], *d)* $A = 10$ MJy sr^{-1} for H_2 S(1), *e)* $A = 10$ MJy sr^{-1} for [S IV], *f)* $A = 30$ MJy sr^{-1} for the 7.7μm PAH band, and *g)* $A = 30$ MJy sr^{-1} for the 11.2μm PAH band. *h)* The CO(1–0) map overlaid on the HST F814W image of the nucleus. Contours are 118 K km s^{-1} $\times(1, 4, 8, 12, 16)$.